DET KGL. DANSKE VIDENSKABERNES SELSKAB
MATEMATISK-FYSISKE MEDDELELSER, BIND XXV, NR. 16

A NEW TYPE OF β-RAY SPECTROGRAPH

BY

O. KOFOED-HANSEN,
J. LINDHARD AND O. B. NIELSEN

KØBENHAVN
I KOMMISSION HOS EJNAR MUNKSGAARD
1950

Printed in Denmark.
Bianco Lunos Bogtrykkeri.

§ 1. Introduction.

In later years several methods of designing magnetic β-spectrographs have been proposed and applied in practice. Among these the most important are the magnetic lens spectrograph used by KLEMPERER (1935) and later on by DEUTSCH, ELLIOTT and EVANS (1944), SIEGBAHN (1943) and others, and the two-directional focusing spectrograph introduced by SVARTHOLM and SIEGBAHN (1946). A modification of the latter spectrograph was built by SNYDER (1948) and used in measurements on protons from nuclear reactions. A spectrograph of the lens type with a special field was recently proposed by RICHARDSON (1949).

It is a common feature of these types of spectrographs that the focusing is obtained only in a first approximation, and since high resolving power is desirable the solid angle of emitted β-particles which could be utilized in the spectrograph had to be small. In fact, there will always be a competition between the resolving power $R = p/\Delta p$ and the effective solid angle, Ω, and the values of these two quantities may for many purposes be taken as a measure of the efficiency of the apparatus, even though other properties like dispersion are of importance. In the best spectrographs one may have, e. g., $1/R \sim 1\,^0/_0$ and $\Omega \sim 1\,^0/_0$ of $4\,\pi$. With refined lens spectrographs it has recently proved possible to attain a further improvement by a factor of 2 (SLÄTIS and SIEGBAHN 1949; see also ZÜNTI 1948, and DU MOND 1949).

The question can now be raised whether it is possible to increase further the transmission by any considerable factor without essential reduction in resolution. This can be brought about only if the β-spectrograph is rather different from the common type, since in principle one must then have exact focusing. It seems reasonable to exclude beforehand spectrographs involving electric fields, since it is much easier to produce

magnetic fields of the order of magnitude demanded in β-spectrographs.

From the experimental point of view the problem of obtaining focusing for a large solid angle is of course always of interest, but it is the more pertinent if one has a β-source of very low intensity. A typical case of this kind arises if one wants to estimate the energy of hard γ-rays from nuclear reactions by measuring the energy of the Compton electrons produced by the radiation. Since the distribution in energy of Compton electrons is comparatively wide, the resolving power need not be very high. On the other hand the intensity is so low that it becomes necessary to focus a considerable fraction of the fast electrons produced.

The present paper is an attempt at solving the problem of focusing for a large solid angle with a magnetic spectrograph. The guiding principles used may be shortly outlined as follows. First of all, it seems natural to demand that the field be cylindrically symmetrical around the line connecting source and focus. We shall further require that each β-particle moves in a plane containing the axis of the spectrograph. The magnetic field must therefore be normal to this plane, which entails that the currents producing the field have component zero perpendicular to the plane. We shall also suppose that the current distribution in a plane containing the axis can be represented by a single closed ringformed current. These requirements make it possible, at least in a first approximation, to build the spectrograph with the use of wedge-shaped pole pieces having plane surfaces, so that the gaps are also wedge-shaped. The edges of the pole pieces will then just correspond to the closed curve describing the associated current. The arrangement of pole pieces and gaps is shown in Fig. 1. With the above conditions the magnetic field will be inversely proportional to the distance from the axis. It may be mentioned that BENDER and BAINBRIDGE[1] have built a spectrograph with one gap, where the magnetic field is inversely proportional to the distance from the centre of the spectrograph. Theoretically, this seems not to give as good possibilities of all-over focusing as the present type.

In the calculation below we shall not in the first instance

[1] We are much indebted to Dr. BAINBRIDGE for information regarding this spectrograph.

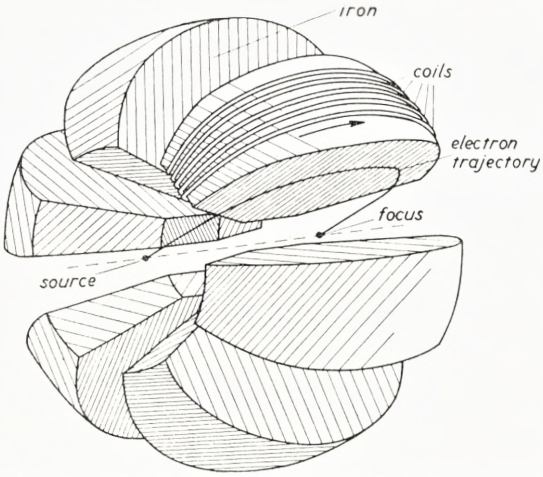

Fig. 1. A schematic illustration of the arrangement of pole pieces and gaps of a symmetrical spectrograph with 6 gaps of opening angle 30°.

discuss the possibilities of constructing magnets giving the desired field. We shall apply instead the idealized picture with a ring current in a plane containing the axis and assume that we can dispose freely of this current and also that it forms no mechanical obstacle to the motion of the β-particles.

It turns out that even with the above limitations there is a great variety of solutions with point focusing for a large solid angle. We have given a detailed description of one particular kind of solution, which besides rotational symmetry shows symmetry with respect to the central plane in the spectrograph. The other types of solutions are accounted for more schematically.

In order to appreciate the advantages or disadvantages of the different solutions it is necessary to obtain estimates of the resolving power of the spectrograph. We have therefore tried to look into the questions of image formation, dispersion and effects of stray fields at the edges of the pole pieces. The above-mentioned symmetrical solution is found to be particularly simple and is the only case with image formation. This is by no means a strong argument against asymmetrical solutions. It seems most important to select only such solutions where the electron trajectories meet the boundary curve at nearly right angles.

A model of the symmetrical spectrograph with only one gap was built, and the focusing and resolution was measured (see

§ 5). This model was found to be in fair accord with theoretical estimates, and as far as the preliminary evidence goes, a spectrograph constructed on these lines can have, e. g., a solid angle $\Omega \sim 20\ ^0/_0$ of $4\,\pi$ and resolving power $1/R \sim 2\ ^0/_0$.

§ 2. The Electron Trajectories.

In this and in the next paragraph the problems of the integration of the equations of motion and the possibilities as to focusing are treated. The discussion is perhaps rather elementary and more detailed than necessary for our purpose. Nevertheless, we considered it of some value to give a comparatively complete account of a treatment which is suited to give the general solution for the kind of spectrograph considered here.

It is convenient to apply cylinder coordinates, where the z-axis passes through source and focus, while r is the distance from the axis, and φ ($0 \leqq \varphi \leqq 2\,\pi$) is the angle of rotation about the axis. As mentioned in the introduction, the current in the z,r-plane is assumed to follow a closed curve, and the component in the direction of φ is zero. In the actual spectrograph this curve describes the boundaries of the pole pieces, in a first approximation at least. The total current in the ring, when integrated over φ, is I e. s. u./sec. It is seen that in the space outside the closed ring the magnetic field is zero and the electrons move in straight lines. Inside the ring the field is

$$H_r = H_z = 0, \quad H = \frac{2\,I}{cr} = \frac{H_1}{r}, \tag{1}$$

where $H_1 = 2\,I/c$ is the field in unit distance from the axis.

Our first step is the integration of the equations of motion for an electron moving in the field given by (1)[1], the motion being confined to the z,r-plane. The radius of curvature of the electron orbits is

$$\left.\begin{aligned} \varrho &= \frac{cp}{eH} = b \cdot r \\ b &= \frac{p \cdot c^2}{2\,eI} \end{aligned}\right\} \tag{2}$$

[1] The motion of electrons in fields of this kind has been treated by Richardson (1947) and applied to β-spectroscopy. However, Richardsons discussion is somewhat different from the present treatment because the application was to a spectrograph similar to the semi-circular type.

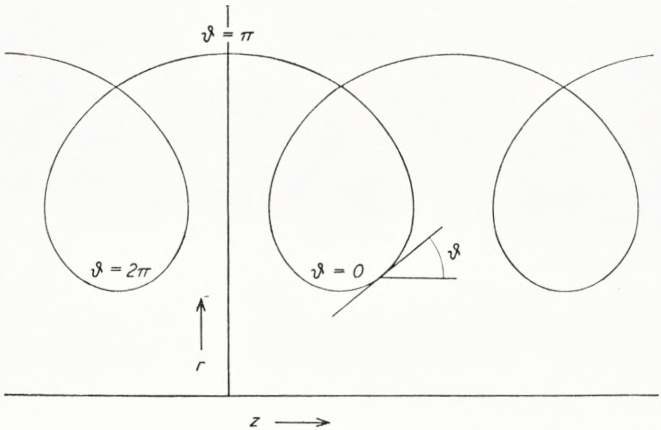

Fig. 2. An electron trajectory in the magnetic field $H = H_1/r$, where the quantity $b = \frac{cp}{eH_1}$ is supposed to have the value 0.6.

and hence ϱ is proportional to r. The constant b depends only on the ratio between the momentum of the electron, p, and the total current, I.

The electron trajectories obey the differential equation

$$\left(1+\left(\frac{dr}{dz}\right)^2\right)^{\frac{1}{2}} = br\frac{d^2r}{dz^2}. \tag{3}$$

This equation is integrated readily and leads to the following expression for z as a function of r

$$z = \int^{r} \frac{\log(y/a)\,dy}{\sqrt{b^2-(\log(y/a))^2}} + z_0. \tag{4}$$

There are two integration constants, a and z_0. In Fig. 2 is shown an electron trajectory, with $b = 0.6$. It is seen that the electrons perform loops, with a drift parallel to the z-axis.

The curves (4) are more conveniently described in a parameter representation with the angle ϑ between the axis and the tangent of the curve as a parameter (see Fig. 2). We write

$$\left.\begin{aligned} z &= ab\,U(b,\vartheta)+z_0 \\ r &= ae^{-b\cos\vartheta} \end{aligned}\right\}, \tag{5}$$

where

$$U(b,\vartheta) = \int_{\pi}^{\vartheta} \cos x\, e^{-b\cdot\cos x}\,dx. \tag{6}$$

We then have $z = z_0$ for $\vartheta = \pi$. It is also seen that the integration constant a simply corresponds to the value of r for $\vartheta = \pi/2$. Moreover, the minimum and the maximum distance from the axis are given by

$$r_{\min} = a \cdot e^{-b}, \quad r_{\max} = a \cdot e^{b}.$$

Therefore, the ratio $r_{\min}/r_{\max}$ is equal to e^{-2b} and does not depend on the constants of integration, but only on the quantity b.

The motion of the electrons was found to be periodic in the direction of the z-axis. From (5) this period is found to be

$$\left.\begin{aligned} z(\vartheta - 2\pi) - z(\vartheta) &= -2\pi\, iab \cdot J_1(ib) = \\ &= 2\pi\, ab^2 (1 + b^2/16 + b^4/192 + \cdots\cdots). \end{aligned}\right\} \quad (7)$$

J_1 is the first order Bessel function of the first kind.

Equation (5) also shows that while b essentially determines the form of the trajectories the integration constant a is a parameter describing a family of curves, similar with respect to the point $z = z_0$ on the z-axis.

The function $U(b, \vartheta)$ defined by (6) can be computed from a suitable series development. For instance, the exponential function in the integrand of (6) may be written as a power series in $b \cos x$, whereby one obtains a rapidly converging series of integrals. However, it seems preferable to use the following series development in Bessel functions

$$\left.\begin{aligned} U(b, \vartheta) &= iJ_1(ib)(\pi - \vartheta) - \\ &- \sum_{n=1}^{\infty} \frac{1}{n} (i)^{n-1} (J_{n-1}(ib) - J_{n+1}(ib)) \sin n\vartheta. \end{aligned}\right\} \quad (8)$$

As will be seen later the values of interest for b will be $b \lesssim 1$. For such values of b it is necessary to retain at most about five or six terms in (8), in order to know U to four decimal places.

In Fig. 3 is shown a set of trajectories, all of them corresponding to the value 1 for b. For all orbits in the figure the maximum value of r corresponds to $z = 0$. This will be called a symmetrical arrangement of orbits all having the same value of b, but different values of a. In Fig. 3 is included only one

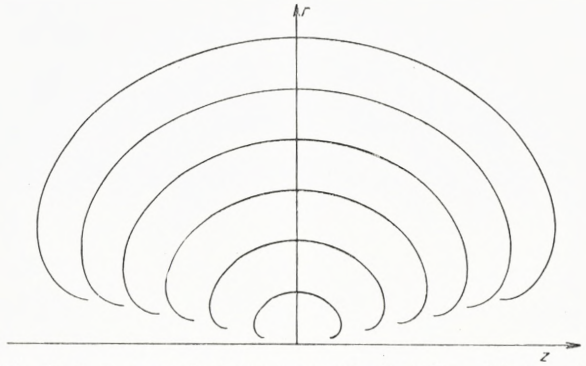

Fig. 3. A symmetrical arrangement of orbits with $b = 1$.

loop in the electron orbits. For obvious reasons the present treatment will be limited to this case, so that $0 \leqq \vartheta \leqq 2\pi$.

Instead of a symmetrical arrangement of orbits we can also pick out a set of orbits for which the z-value corresponding to $r = r_{\max}$ is a function of $r_{\max}$, i. e., a function of a. Any set of orbits of this kind can be characterized by the function

$$\zeta(a) \equiv z(r = r_{\max}). \tag{9}$$

The function $\zeta(a)$ is uniquely defined apart from an arbitrary constant. In the case of a symmetrical arrangement of orbits we may write

$$\zeta(a) = 0. \tag{10}$$

The equations (5) can now be rewritten on the form

$$\left.\begin{aligned} z &= ab\,U(b, \vartheta) + \zeta(a) \\ r &= a\,e^{-b\cos\vartheta}. \end{aligned}\right\} \tag{11}$$

When the function $\zeta(a)$ is chosen the two-parameter family of curves in (5) is replaced by a family depending on only one parameter, a. This representation also corresponds to the point of view to be taken in the following. We choose some one-parameter family of trajectories described by a function $\zeta(a)$ and will then look for the possibilities of obtaining focusing with this family.

§ 3. The Focusing.

Having solved the equations of motion for electrons in the space inside the boundary curve we may proceed to discuss the conditions to be fulfilled by this curve in order that focusing is obtained in a point on the z-axis.

Suppose that β-particles are emitted from a point $z = z_f$ on the z-axis. It is also assumed that we have chosen some one-

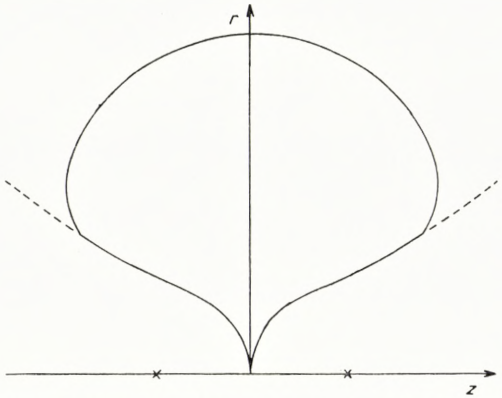

Fig. 4. The figure shows the boundary curve of a symmetrical spectrograph ($z_{f1} = z_{f2}$) with $b = 0.6$. Source and focus are indicated by crosses. Electrons emitted from the source at an angle less than 36° do not meet the boundary curve and can not be focused.

parameter family of curves as described by (11). We then draw the tangents from z_f to each of the curves (11). This is always possible since ϑ varies between 0 and 2π on all curves. Indeed, there will be two tangents for each curve but we choose the tangent on the source side, or the one for which $0 < \vartheta < \pi$. The new curve formed by the touching points of the tangents is just the boundary curve we are looking for, since it corresponds to the edges of the pole pieces of the idealized spectrograph. Inside this curve the magnetic field should be different from zero and the orbits as in (11) while outside we assumed rectilinear motion of the β-particles and a magnetic field equal to zero.

To a point (z, r) is associated a trajectory (11) passing through the point. If the point is to lie on the boundary curve, the tangent

of the trajectory in (z, r) must pass through the source (z_f, o) or

$$\operatorname{tg} \vartheta = \frac{r}{z - z_f}. \tag{12}$$

Together, (11) and (12) therefore give a parameter representation of the boundary curve, and it is most convenient to consider ϑ, and not a, as the parameter. If ϑ is the parameter, we may take (12) as a relation determining a as a function of ϑ; the

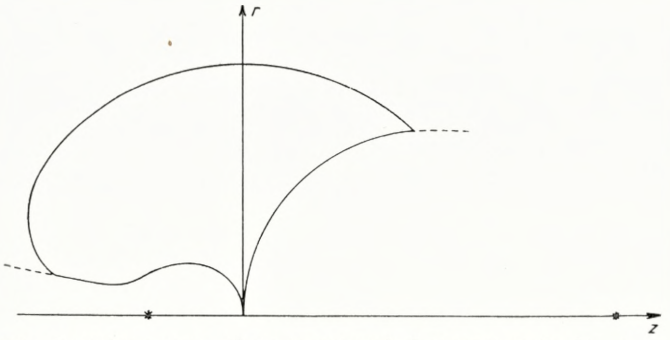

Fig. 5. The boundary curve of an asymmetrical spectrograph ($z_{f1} \neq z_{f2}$) with $b = 1$ and with a symmetrical arrangement of orbits ($\zeta(a) = 0$).

value of a can then be introduced in (11), whereby finally the coordinates (z, r) of the boundary curve are found as functions of ϑ.

Only if $\zeta(a)$ is a simple function will it be easy to give an explicit formula for (z, r). In case $\zeta(a)$ is proportional to a, $\zeta(a) = C \cdot a$, we find

$$\left.\begin{aligned} z &= z_f \cdot \frac{b \cdot U(b, \vartheta) + C}{b \cdot U(b, \vartheta) + C - \cot \vartheta \cdot \exp\{-b \cdot \cos \vartheta\}}, \\ r &= z_f \cdot \frac{\exp\{-b \cdot \cos \vartheta\}}{b \cdot U(b, \vartheta) + C - \cot \vartheta \cdot \exp\{-b \cdot \cos \vartheta\}}, \\ \zeta(a) &= C \cdot a. \end{aligned}\right\} \tag{13}$$

The symmetrical arrangement of orbits corresponds to $C = 0$. As could be anticipated, for $\zeta(a) = C \cdot a$ different values of z_f only lead to boundary curves similar with respect to the origin.

With a given value b it is therefore possible to give once and for all the solution when $\zeta(a) = C \cdot a$, if only the function $U(b, \vartheta)$ is evaluated for this particular value of b. Of course, it holds generally that $U(b, \vartheta)$ is the basic function to be calculated when a boundary curve is desired.

Fig. 4 and 5 show the boundary curves with symmetrical arrangement of orbits in the two cases $b = 0.6$ and $b = 1$. As coordinates are used z/z_f and r/z_f.

Fig. 4 represents a symmetrical arrangement of orbits and the boundary curve is also symmetrical. Evidently, even with the symmetrical arrangement of orbits it is not necessary to have a symmetrical boundary curve. An asymmetrical spectrograph is obtained as soon as the z_f's corresponding to source end and focus end are chosen to be different; this case is illustrated in Fig. 5.

As indicated in Fig.s 3, 4, and 5 only part of the total solid angle can be utilized. If θ is the angle between the positive direction of the z-axis and a straight line through z_f there will be a certain critical angle θ_c defined by the common tangent of the curves (13). Electrons emitted from the source with angles $\theta \leq \theta_c$ can never enter the field and be focused. In the symmetrical case and for b equal to 1 and 0.6, respectively, the critical angles are $\sim 12°$ and $\sim 36°$. This also illustrates the variation of θ_c with b.

Of course, even for angles somewhat larger than θ_c will the trajectories meet the boundary curve at nearly glancing incidence, and it becomes practically impossible to focus the electrons emitted from the source, especially in view of the effects of stray fields occurring at the edges of the pole pieces. This is one of the reasons why in the final spectrograph the cut-off angle must be chosen much larger than θ_c. The angle θ_c will then be of no significance and may be left out of the discussion. We notice that the variation of θ_c with b shows that the larger is chosen the value of b the easier it will be to focus β-rays ejected in backward directions, i. e., with θ small.

In the calculations on the boundary curve we found that there is a large freedom in the choice of the following variables: the distance between source and focus, the boundary curve, the function $\zeta(a)$, the field strength, etc. To put it more definitely we can dispose rather freely of the quantity $b = p \cdot c^2/2\,eI$, the coordinates

of source and focus and at the same time of e. g. the function $\zeta(a)$. The boundary curves at the focus and source end are then determined from these variables. Of course, we may instead choose one of the boundary curves and with this choice find the corresponding function $\zeta(a)$ and the other boundary curve. Finally, the opening angles of the wedge shaped gaps and of the pole pieces are left undetermined so far.

The freedom of choice as expressed by these variables is rather convenient, because the calculations below on focusing and resolving power lead to several restrictions e. g. as regards the form of the boundary curve. Here, the primary condition is that both resolution and effective solid angle are sufficiently large. When these conditions are fulfilled one is still left with several possibilities. The choice between these possibilities will depend on the more technical aspects of the problem.

In the kind of solution considered here the total angular deflection of the orbits is less than 2π. One might also consider solutions where the trajectories perform several loops of the kind shown in Fig. 2 before being focused. The boundary curves will then be somewhat different from those considered here, but they are easily obtained from the present curves. In this connection it may be mentioned that in the present solution many electrons of low energy meeting the boundary curve on the source side may pass through the field performing a number of loops on the way. They will then leave the field in a more or less random direction at the focus end. These electrons, therefore, will give rise to a background, which may be inconvenient. However, spurious effects of this kind can be removed by suitable screening devices.

§ 4. Image Formation, Dispersion and Resolving Power.

In this paragraph we shall treat questions connected with the resolving power of the β-spectrograph. It is well known that in the usual spectrographs with first order focusing there is a very direct competition between the resolving power, R, and the effective solid angle, Ω, utilized in the spectrograph. However, in the type of spectrograph discussed here, with focusing for a large

effective solid angle, the resolution R is more independent of the effective solid angle and can in fact be made quite large. One might say that the spectrograph consists of a number of small spectrographs, each of these corresponding to one of the wedge-shaped gaps so that the possibility of an improvement as regards resolution and solid angle is due to the replacement of one spectrograph by several. As we shall see, such a description can be justified from the fact that while the idealized spectrograph has an infinitely good resolution and corresponds to an infinite number of gaps, the imperfections arise from the number of gaps being limited, whereby the rotational symmetry is violated.

As a preliminary to the discussion of resolution we shall treat the question of image formation. We consider first an electron which, though moving in the z, r-plane, is not emitted from the source point $(z_{1f}, 0)$ but from a point in the immediate neighbourhood of this space point. The variables on the source side of the spectrograph are given the index 1. Let us choose a point (z_1, r_1) on the boundary curve. This point as determined by (11), (13), is a function of ϑ, or, as is convenient in the present case, a function of the parameter a. At the same time, the boundary curve is completely determined from the function $\zeta(a)$ and the value of z_{f1} and b.

Suppose that the electron arrives at (z_1, r_1). If the electrons from the source $(z_{f1}, 0)$ arrive at an angle ϑ_1, the electron considered must pass at a slightly different angle $\vartheta_1 + \delta\vartheta_1$ where $\delta\vartheta_1$ is a function of ϑ_1. Now, since the further motion in the proper trajectory of the electron is described by $\zeta(a)$, as giving the abscissa for the maximum value of r, the slightly changed orbit will be defined by the new ζ-function, $\zeta(a) + \delta\zeta(a)$. We therefore calculate first the change $\delta\zeta(a)$ as a function of $\delta\vartheta_1(\vartheta_1) = \delta\vartheta_1(a)$, remembering that ϑ_1 and a are connected by a one-to-one correspondence. In order to find $\delta\zeta(a)$ we perform a variation calculus in equation (11), varying $\zeta(a)$, a, and ϑ_1, while the point (z_1, r_1) and of course also b are kept fixed. With this procedure we obtain (see Fig. 6)

$$\delta\zeta(a) = \delta\vartheta_1(a) \cdot b \cdot \left(z_{f1} - \zeta(a) + a \cdot \frac{d}{da}\zeta(a) \right) \cdot \sin\vartheta_1 . \qquad (14)$$

Now, we are of course not much interested in the actual values of $\delta\zeta(a)$, since we only want to find the new trajectories in the focus end. Let the variables at the focus end be given the index 2. We shall further use the convention that while the positive direction of the z-axis on the source side is taken from focus to source the positive direction on the focus side is opposite, or from source to focus. This will mean that all formulas between

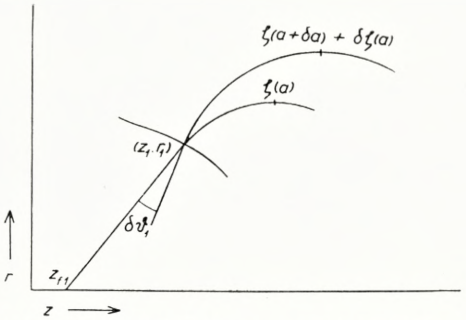

Fig. 6. An illustration of the calculation on image formation. A β-ray entering at an angle $\vartheta + \delta\vartheta_1$ slightly different from that corresponding to focusing. The parameter a and the function $\zeta(a)$, defining the trajectory, are thereby changed.

variables on the focus side are found from those on the source side simple by changing the indices from 1 to 2, and by replacing $\zeta(a)$ by $-\zeta(a)$. This gives immediately the formula corresponding to (14), and the connection between $\delta\vartheta_1(a)$ and $\delta\vartheta_2(a)$ is then

$$\left.\begin{aligned} &\sin\vartheta_2 \cdot \left(z_{f2} + \zeta(a) - a \cdot \frac{d}{da}\zeta(a)\right)\delta\vartheta_2(a) = \\ &-\sin\vartheta_1 \cdot \left(z_{f1} - \zeta(a) + a \cdot \frac{d}{da}\zeta(a)\right)\delta\vartheta_1(a). \end{aligned}\right\} \quad (15)$$

In principle formula (15) describes the new trajectories on the focus side, as corresponding to, e. g., particles coming from a point in the neighbourhood of the source. However, a formula like (15) is rather difficult to handle. In the simplest case, that of the symmetrical spectrograph where $\zeta(a) = 0$, $z_{f1} = z_{f2}$ and $\vartheta_1(a) = \vartheta_2(a)$, it is immediately seen that $\delta\vartheta_1(a) = -\delta\vartheta_2(a)$. This means that there will be first order image formation and the magnification is 1.

The treatment so far relates only to particles moving in the z, r-plane. It is necessary to consider trajectories which are not contained in a plane through the symmetry axis. From conservation of momentum about the axis it follows that a particle passing the axis at a small distance d_1 on the source side, in the focus end will pass at a instance d_2 on the opposite side of the axis, where

$$d_1 \sin \vartheta_1 = d_2 \sin \vartheta_2, \tag{16}$$

ϑ being the angle between the trajectories and the axis. The radial motion of the particle and the connection between ϑ_1 and ϑ_2 remains the same as that described in (15).

Again, in the case of the symmetrical spectrograph where $\vartheta_1 = \vartheta_2$ formula (16) shows that the above mentioned image formation holds true for all directions of emission from a point in the neighbourhood of the source. Moreover, the completely symmetrical spectrograph is the only kind having the property of image formation. We shall not give the proof of this result here; it follows from simple consideration using equations (15) and (16). The property of image formation might seem to imply a special advantage of the symmetrical spectrograph over other types. In how far this property is of importance to the actual spectrograph will be discussed in connection with the resolving power.

In order to find the dispersion of the spectrograph we consider the motion of particles with energies differing slightly from that corresponding to focusing. The effect resulting from a change in energy may also be obtained through a change in the magnetic field, because it only depends on the change δb of the quantity $b = p c^2/2 eI$.

As above the trajectory is supposed to pass through a point (r_1, z_1) at the source end. Keeping z_1, r_1 and ϑ_1 fixed, which means that the particle comes from the source $(z_{f1}, 0)$ the quantities b, a and $\zeta(a)$ in (11), (13) are varied. The variation gives $\delta\zeta(a)$ as a function of δb and a on

$$\left.\begin{aligned} \delta\zeta(a) = -\delta b \Big\{ & ab \cos\vartheta_1 \, U(b, \vartheta_1) + aU(b, \vartheta_1) + \\ & + ab \frac{\partial}{\partial b} U(b, \vartheta_1) + a \cos\vartheta_1 \frac{d}{da} \zeta(a) \Big\}. \end{aligned}\right| \tag{17}$$

From $\delta\zeta\,(a)$ the varied motion in the focus end is calculated in a similar way as in the treatment of image formation. It is then found that the new path through the point (z_2, r_2) on the boundary will leave at the changed angle $\vartheta_2 + \delta\vartheta_2$, given by

$$\left.\begin{aligned}\delta\vartheta_2 \left\{\sin\vartheta_2\, b\frac{d}{da}\zeta\,(b) - b^2\,U\,(b\,,\,\vartheta_2)\sin\vartheta_2 + b\cos\vartheta_2\, e^{-b\cos\vartheta_2}\right\} = \\ = -\delta b\left\{U\,(b\,,\,\vartheta_1) + U\,(b\,,\,\vartheta_2) + bU\,(b\,,\,\vartheta_1)\cos\vartheta_1 + bU\,(b,\,\vartheta_2)\cos\vartheta_2 + \right. \\ \left. + (\cos\vartheta_1 - \cos\vartheta_2)\frac{d\zeta\,(a)}{da} + b\frac{\partial}{\partial b}(U\,(b\,,\,\vartheta_1) + U\,(b,\,\vartheta_2))\right\}.\end{aligned}\right\} \quad (18)$$

It is to be remembered that ϑ_1 and ϑ_2 are the ϑ-values at two points on the two boundary curves, belonging to the same unvaried trajectory. Moreover, the variation δb of b is connected with the variation δp of the momentum through the relation $\delta b/b = \delta p/p$, and this is also approximately equal to $\delta E/E$ if the electrons have relativistic energies.

In the case of the completely symmetrical spectrograph (18) reduces to

$$\delta\vartheta_2 = -\frac{2\,\delta b}{b}\cdot\frac{a}{\sin\vartheta\cdot z_f}\left\{\cos\vartheta\cdot bU\,(b\,,\,\vartheta) + U\,(b\,,\,\vartheta) + b\frac{\partial}{\partial b}U\,(b\,,\,\vartheta)\right\}. \quad (19)$$

One can instead characterize the varied path by the shortest distance δx between the focus and the path. The quantity δx may be called the linear dispersion, and the ratio $\delta x/z_f$ divided by $\delta p/p$ the dispersion factor. The dispersion is easily calculated from (19) and in Table I is tabulated the dispersion factor as a function of ϑ_1 in the case of $b = 0.6$ and for $60° < \vartheta < 150$. This gives a direct illustration of the shift of the trajectory when the energy is changed. For comparison, the corresponding displacement in the semi-circular spectrograph is given by the dispersion factor $f = (\delta x/z_f):(\delta p/p)$ being equal to 2. It is therefore seen that in the present case the dispersion in a reasonably large angular interval is of the order of or larger than that in the semi-circular spectrograph.

So far, we have discussed only image formation and dispersion

Table 1.

The table gives the dispersion factor $f = (\delta x/z_f):(\Delta p/p)$ as a function of ϑ for $b = 0.6$ and $\zeta(a) = 0$. In the same units the dispersion factor of the semicircular spectrograph is $f = 2$.

ϑ	dispersion factor
60°	21
75°	9.1
90°	5,1
105°	3.3
120°	2.8
135°	1.8
150°	.3

in the idealized field. Now, the actual resolution will be determined essentially by two kinds of imperfections.

First, the device for collecting and recording of the β-rays at the focus has a finite extension and will on account of the dispersion registrate particles in a finite energy interval, ε. It is even desirable that particles in a not too small energy interval are counted because the intensity thereby becomes larger. If the dimensions of the collector are $\sim \lambda$ the resolving power resulting from this effect will be of the order

$$R_d = \frac{p}{\Delta p} \sim \bar{f}\frac{\lambda}{z_f} \tag{20}$$

where $\bar{f}$ is an averaged value of the dispersion factor f.

The second imperfection is due to deviations from axial symmetry of the actual field. This gives rise to a finite resolution R_r, and the total resolution will then be a function of R_d and R_r. It is desirable that the comparatively simpler of the two, R_d, gives the smaller contribution to the final resolution, so that

$$R_d \gtrsim R_r \quad \text{and} \quad R \approx R_r .$$

The effects of stray fields on the focusing may be estimated as follows. Suppose that the pole edges are nearly straight lines and that the pole faces are approximately parallel. The extension of the fringing field beyond the edges will then be of the order

of the width of the gap (compare e. g. COGGESHALL 1947) and therefore of the first order in Φ, the opening angle of the gap. The fringing field will have a component parallel to the gap and normal to the boundary curve, besides the component normal to the gap. It will then have mainly two effects on the motion of the β-particles.

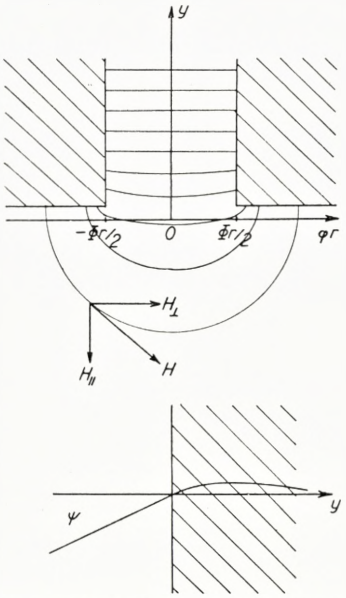

Fig. 7. The effect of the fringing field. The upper figure sketches a section perpendicular to the gap. The distance from the centre of the gap is measured in units φr, r being constant. As illustrated in the lower figure ψ is the angle between the trajectory and the normal of pole boundary.

First, there will be an extra deflection of the β-rays parallel to the plane of the gap. The angular deflection in this plane may be written as (see Fig. 7)

$$\Delta\vartheta = \frac{e}{pc}\int H_{\perp}\, dy \cdot \frac{1}{\cos\psi} = \frac{\alpha \cdot \Phi}{b\cos\psi} \sim \Phi. \qquad (21)$$

Here, ψ is the angle between the trajectory and the normal of the boundary; α is a constant, $\alpha \lesssim 1$, defined by $\int H_{\perp}\, dy = \alpha\, H_0\, r\, \Phi$ where $r\,\Phi$ is the width of the gap. It is noteworthy that

$\Delta\vartheta$ is independent of φ. The effective shift of the boundary curve as estimated in this way $\sim \alpha \cdot r \cdot \Phi$.

The second effect is the deflection normal to the gap, which is brought about by the component of the field parallel to the gap. This deflection is not the same all over the gap, and will be greatest close to the pole faces. We may approximately write $\int H_{||}\, dy = H_0\, r\, \varphi$ and find then for the angular deflection

$$\Delta w = \frac{e}{pc} \int H_{||}\, dy \operatorname{tg} \psi \gtrsim \frac{\varphi\psi}{b}. \tag{22}$$

Since in the gap $\varphi \leq \Phi/2$, the deflection is of the first order in Φ, and at the same time proportional to the angle ψ between the trajectory and the normal of the boundary.

Now, there will be two deflections of this kind, one at either boundary curve, and as a rule these two deflections will be to the same side. This holds for instance in the completely symmetrical spectrograph, if the first deflection is not so large as to bend the trajectory into the other side of the gap.

In order to find the total shift of the trajectory at the focus we may, as in equation (16), find the angular momentum about the axis given to the particle by the deflections. We then find from (22) that the trajectory passes the focus at a distance d from the axis, given by

$$d \sin \vartheta_2 \gtrsim \frac{r_1 \varphi_1 \psi_1 + r_2 \varphi_2 \psi_2}{b} < r\psi\Phi/b\,. \tag{23}$$

At the same time the requirement that a negligible number of the particles e. g. are deflected and hit the pole faces is approximately equivalent to saying that $\psi \ll 1$. From these results it therefore seems most important that ψ is much smaller than 1, i. e., the trajectory should be closely normal to the boundary curve. It is noteworthy that the first order defocusing effect is normal to the axis and not parallel to it. The formulas (22) (23) give a rough estimate of this effect.

In these considerations it was assumed that the fringing field is of small extension. However, it must be remembered that though the fringing field is weak at large distances from the edges

the summed-up effects on the trajectories of the field far from the edges is not completely negligible (COGGESHALL 1947). Moreover, other imperfections as the fringing fields at the outer pole boundaries will entail corrections to the inner boundary curve. We must accordingly expect that the above results as regards defocusing effects can only give an indication of the effect on the trajectories of the opening angle of the gaps being finite.

§ 5. Preliminary Experimental Investigation.

The above theoretical discussion served the following purposes. First, to find the freedom of choice of the variables pertaining to the spectrograph and to make possible approximate calculations of the shape of the pole pieces. Second, through qualitative considerations to obtain an insight in the questions of dispersion, resolving power, etc., in order to have some guidance as regards the choice of the shape of the boundary curve and similar factors.

With the results found in the theoretical treatment one should have a reasonable starting point for the experimental investigation. It was found most profitable to build first a single gap. In this way the theoretical results could be controlled and improved upon. As we shall see, even the one-gap spectrograph shows an appreciable solid angle, and it compares favourably with other spectrographs. Still, it must be remembered that in the case of a single gap the field need not be exactly the same as that in the final spectrograph with many gaps, and some differences may be found at the edges of the pole pieces. With such reservations we shall consider the single gap to give a fair account also of the properties of the spectrograph with many gaps. In particular, the one-gap spectrograph will indicate whether the large value of Ω promised by the theory may be realized.

It was decided to construct a completely symmetrical spectrograph. The form of the boundary curve describing the edges of the pole pieces is then determined by the choice of the value of b. The b-value used was $b = 0.6$. With this values of b and with focusing in the angular interval $75° \lesssim \vartheta \lesssim 135°$ the boundary curve was expected to become nearly perpendicular to the

electron trajectories. The distance between source and focus was chosen to be $2\,z_{f1} = 12$ cm. Two different gaps of the described kind were used; one with an opening angle between the pole pieces of 18°, and the other with opening angle 30°. The maximum solid angle one could hope to utilize in the one-gap models was then 3 % and 5 %, respectively.

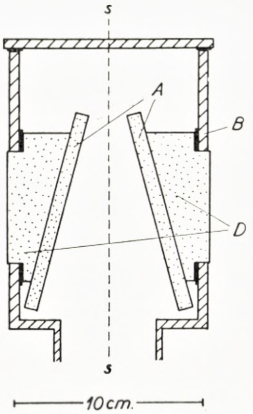

Fig. 8. A section through the 30° one-gap model, perpendicular to the axis.

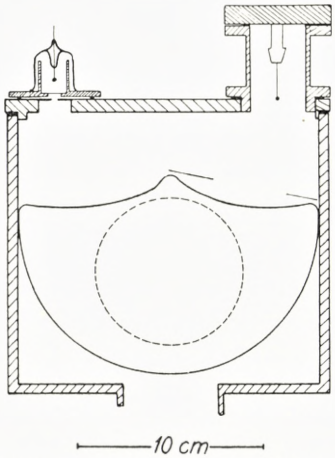

Fig. 9. A section parallel to the axis of the 30° model showing source, focus and one of the pole pieces.

The apparatus is illustrated in Fig.s 8 and 9. As shown in Fig. 8 the pole pieces are two plane parallel iron plates, *A*, of thickness 7 mm. The plates are mounted on two cylindrical iron blocks, *D*, the outer surfaces of which are joined to the pole pieces of an electromagnet. This set-up is placed in a brass vacuum chamber, *B*. In Fig. 8 the angular gap between the pole pieces is seen to be 30°. The model with opening angle 18° is quite similar to the 30°-model illustrated in Fig.s 8 and 9. Fig. 9 shows a cut through the central plane of the chamber, corresponding to the line *s-s* in Fig. 8. At the top of the chamber is an opening, where the source is placed, and at the other end a window corresponding to the focus.

At the bottom is a connection to an oil pump. The pressure is measured by means of a Pirani manometer; the pressures used were of the order of 10^{-2} mm Hg. In Fig. 9 are further

seen the edges of the pole pieces and at the source side a movable aluminium plate with a diaphragm. Since the diaphragm allowed only the passage of limited beams of electrons the focusing for the different trajectories could be measured separately.

The source consisted of a small sample of *Th B* placed on a copper sphere of diameter 1.5 mm. The *F* line of *Th B* of energy 146 keV was used in the measurements. It was possible to focus β-particles of energies up to about 5 MeV. The G.-M. counter was connected to an amplifier, a scale of 32, and a recording arrangement. The source could easily be placed at different points in the neighbourhood of the theoretical source point. The slit at the focus below the counter could also be moved and was in some of the measurements replaced by a small circular hole.

The edges of the pole pieces were formed in accordance with the theoretical boundary curve and without corrections for the effect of the fringing fields, even though such effects could be estimated in a qualitative way.

After the mounting of the apparatus the focusing properties were found by scanning the spectrograph with the *Th B* β-rays by means of the movable aluminum plate with a diaphragm. For each angle, ϑ, of emission of the β-rays was determined the current J', in the coils of the electromagnet giving focusing in the slit placed at the theoretical focus. In this way one found J', as a function of ϑ, as shown by the dotted curve in Fig. 10. Evidently there will be complete focusing only when J', is a constant. From these measurements it was possible to find the corrections to be made on the edges of the pole pieces. In Fig. 11 is seen the profile of a pole piece. The dotted curve is the uncorrected boundary curve, while the full-drawn line corresponds to corrected curve. One might perhaps at first sight expect that the correction should only correspond to a slight upward shift of the boundary curve as a whole, caused by the stray fields extending somewhat beyond the edges. The actual corrections are somewhat different. At the outer edges there is even an addition of iron. The reason for this is that the outermost orbits of the β-particles lie close to the upper edges of the pole pieces and the field is here slightly weaker than the ideal field because of the boundary effects. Further, the inward displacement of the

edges in the middle of the spectrograph is considerable. The main part of this displacement had a special origin, for the surface of the iron blocks holding the pole pieces lies quite close to the boundary curve, as seen from Fig. 9, and therefore the additional stray field between the blocks gave rise to a disturbance. In the model with a gap of 18°, this disturbance was reduced somewhat by removing a part of the blocks, but

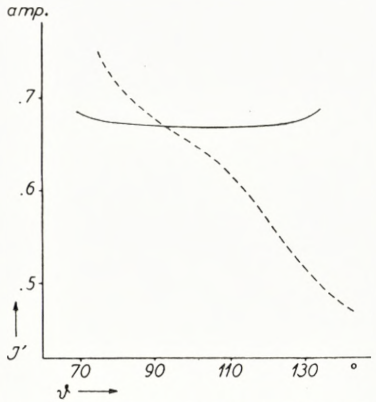

Fig. 10. The current, J', in the electromagnet corresponding to focusing of the *Th B F*-line, as a function of the direction of emission of the β-rays, ϑ. The dotted and the full-drawn lines, respectively, correspond to the uncorrected and the corrected pole pieces.

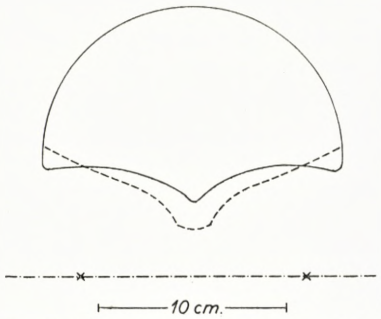

Fig. 11. The figure shows the uncorrected pole pieces (dotted line) and the corrected pole pieces (full-drawn line).

apart from this it was not found worth while to make further corrections of this kind in the preliminary investigation.

With the corrected pole pieces the current J' in the magnet was again found as a function of ϑ. This current is given by the full-drawn curve in Fig. 10 and is very nearly constant in the region $75° \lesssim \vartheta \lesssim 130°$. The corrected pole pieces were therefore considered satisfactory and a more thorough investigation of resolution and focusing was carried through.

In the measurement on resolution the abovementioned diaphragm was so placed as to give a beam of β-particles normal to the edges of the pole pieces. Below the counter at the focus was a slit of width 0.7 mm. The resolution was determined from the width at half peak height of the *F* line of *Th B*. Fig. 12 shows

the β-spectrum of *Th B* in the neighbourhood of this line, as measured with the gap of opening angle 18°. The diaphragm allowed a beam corresponding to 0.7 % of the total solid angle and as seen from Fig. 11 the resolving power was $1/R \sim 1.3$ %. The total gap was estimated to have $\Omega \sim 3$ % and $1/R \sim 4$ %. There seems to be a possibility of considerable improvement of these results, the more so because the pole pieces in the 18°-gap

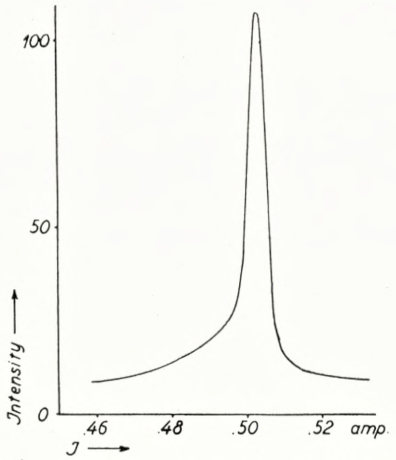

Fig. 12. The *F* line of *Th B* as measured with the 18° one-gap model.

were not corrected in this gap, but were formed as those corrected in the 30°-gap.

With the diaphragm at the source end in the same position the focusing in two directions was investigated. For this purpose the slit at the focus was replaced by a circular diaphragm of diameter 2.5 mm. The diaphragm could be moved perpendicular to the central plane of the gap. For each of a number of positions of the diaphragm was found a curve like that in Fig. 12, giving the intensity of β-particles passing through the diaphragm as a function of the current in the electromagnet. The maximum value of the intensity for each position was determined, and in Fig. 13 these maximum values are plotted as a function of the distance $\Delta_\perp$ between the centre of the diaphragm and the axis of the spectrograph. The different maximum values of intensity were all found to correspond to the same current J' in the elec-

tromagnet. Considering that the diameters of the diaphragm and of the source are 2.5 and 1.5 mm. the curve in Fig. 13 shows that the focusing is good in the direction perpendicular to the central plane of the gap. As expected the spectrograph therefore shows two-directional focusing.

Similar measurements were performed for other sections of the solid angle subtended at the source, and it was found that

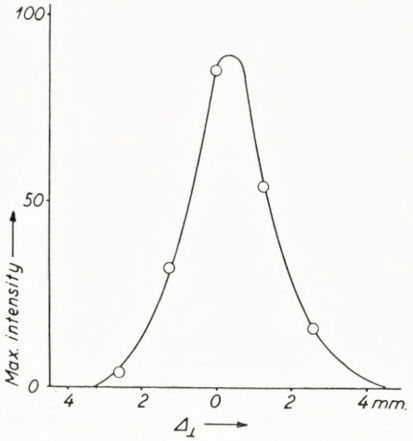

Fig. 13. The focusing perpendicular to the axis in the 18° one-gap model. As abscissa is used Δ_1, the distance from the axis. The ordinate is the maximum intensity through the diaphragm at the distance in question.

in those parts where the trajectories of the β-particles are not perpendicular to the edges of the pole pieces the focusing in the direction normal to the central plane of the gap was markedly inferior. The total width of the curve corresponding to the one in Fig. 13 was in the most unfavourable case as large as ~ 10 mm. According to the considerations in § 4 a pronounced defocusing effect should come in when the trajectories meet the edges of the pole pieces at oblique incidence. Even more quantitatively formula (23) seems in agreement with the defocusing effect measured.

These preliminary measurements indicate that even the very simple one-gap spectrograph can be used to advantage in β-spectroscopy. They also seem promising with respect to the final spectrograph with many gaps. It is planned to build a minor spectrograph of this kind. For instance, it may consist of 6 gaps

of opening angle 18°, which would lead to a maximum solid angle of about 20 %.

Summary.

An axially symmetric β-spectrometer with source and focus outside the magnetic field is discussed, the advantages of the type chosen being large solid angle and a considerable number of different solutions with focusing. The actual spectrograph will contain many gaps between pole pieces with plane faces. With a suitable choice of the boundaries of the pole pieces the effects of fringing fields can be reduced.

The properties of a very crude model with one gap was investigated and it showed agreement with the theory. The final spectrograph with 6 gaps is expected to have a solid angle of about 20 %.

Institute for Theoretical Physics,
University of Copenhagen,
Denmark.

References.

COGGESHALL, N. D., 1947, Journ. Appl. Phys. **18**, 855.

DEUTSCH, M., ELLIOTT, L. G., and EVANS, R. D., 1944, Rev. Sc. Inst. **15**, 178.

DUMOND, J. W. M., 1949, Rev. Sci. Inst. **20**, 160, 616.

KLEMPERER, O., 1935, Phil. Mag. **20**, 545.

RICHARDSON, H. O. W., 1947, Proc. Phys. Soc. London **59**, 791.

RICHARDSON, H. O. W., 1949, Phil. Mag. **40**, 233.

SIEGBAHN, K., 1942, Arkiv f. mat., astr. o. fys. Bd. **28** A, No. 17.

SLÄTIS, H. and SIEGBAHN, K., 1949, Phys. Rev. **75**, 1955.

SNYDER, C. W., 1948, Thesis, California Institute of Technology.

SVARTHOLM, N. and SIEGBAHN, K., 1946, Arkiv f. mat., astr. o. fys. Bd. **33** A, No. 27.

ZÜNTI, W., 1948, Helv. Phys. Acta. **21**, 179.

Indleveret til selskabet den 9. december 1949.
Færdig fra trykkeriet den 21. april 1950.